*SUPPORTING INFORMATION*
*for*

# ATPase active-site electrostatic interactions control the global conformation of the 100 kDa SecA translocase.

**Dorothy M. Kim [1,2], Haiyan Zheng [3,4], Yuanpeng J. Huang [3], Gaetano T. Montelione [3,4], and John F. Hunt [1]***

[1] Department of Biological Sciences, 702A Fairchild Center, MC2434, Columbia University, New York, NY 10027, USA;

[2] Departments of Biochemistry and Molecular Biophysics, Columbia University,

650 West 168th Street, New York, NY 10032, USA;

[3] Center for Advanced Biotechnology and Medicine, Department of Molecular Biology and Biochemistry, and Northeast Structural Genomics Consortium, Rutgers, The State University of New Jersey, Piscataway, New Jersey 08854;

and

[4] Department of Biochemistry and Molecular Biology, Robert Wood Johnson Medical School, University of Medicine and Dentistry of New Jersey. Piscataway, New Jersey 08854.

* Corresponding author: (212)-854-5443 voice; (212)-865-8246 FAX; jfhunt@biology.columbia.edu.

## Running Title: Active-site electrostatic interactions control SecA conformation

*Version 5.0: Tuesday, October 30, 12 @ 3:36 PM.*

# Supporting Methods

***Cloning and mutagenesis.*** Constructs were described by Weinkauf *et al*. [1]. Point mutations were introduced by PCR using the Stratagene Quikchange kit (Stratagene, La Jolla, CA). PCR products were cleaned by the Qiagen PCR purification kit (Qiagen, Frankfurt, Germany) and transformed into *E. coli* DH5α competent cells. Single colonies were grown in Luria-Bertani broth overnight, and plasmid DNA was extracted from cells by the Qiagen Spin Miniprep kit. Purified plasmids were sequenced by Genewiz, Inc. (South Plainfield, NJ).

***SecA protein expression and purification.*** *E. coli* SecA constructs were transformed into BL21.19 temperature-sensitive expression cells, and *B. subtilis* SecA constructs were transformed into pLysS cells. A single colony was used to inoculate a 150 mL culture of LB with ampicillin (and chloramphenicol in pLysS cells) and grown with aeration overnight at 37 ºC. 10 mL of the overnight culture was used to inoculate a 1 L culture containing LB and supplemented with LinA salts. 12 L of cultures were grown to an O.D. of 0.8-1.0 and then induced with 2 mM IPTG for 16 hours at 20-25 ºC. Cells were spun at 4000 rpm for 20 minutes and the pellets were resuspended with wash buffer (50 mM Tris-HCl pH 7.6, 100 mM NaCl, 1 mM DTT, 1 mM EDTA, 1 mM PMSF). The supernatant was discarded and the cells were resuspended in wash buffer + 20% glycerol, flash frozen in liquid nitrogen and stored at -80 ºC. Cells were lysed and purified as previously described [1], and a gel-filtration step was added using a Sephacryl-300 column (GE) in either TKM buffer for enzymology or crystallization buffer (20 mM BES pH 7.0, 300 mM $Am_2SO_4$, 1 mM DTT) for crystallization studies. Fractions containing SecA were pooled and concentrated using an Amicon-50K centrifugation device to 20 mg/ml for crystallization or 1-5 mg/ml for enzymology, aliquoted and snap-frozen.

***MjDEAD protein expression and purification.*** A pET-28 vector (Novagen) containing *mj0669* was used to express N-terminally His-tagged WT and E155Q-*Mj*DEAD in Rosetta (DE3) cells (Novagen). Cells were grown in Terrific Broth containing 50 ug/ml kanamycin and induced at an $OD_{600}$ of 0.6 with 1 mM IPTG for 16 hours at 20 ºC. Harvested cells were lysed by high pressure emulsion in 50 mM Tris-HCl pH 7.5, 500 mM $NH_3(SO_4)_2$, 10% glycerol, 0.02 % $NaN_3$, and 5 mM DTT. The resulting lysate was centrifuged for 1 hour at 17,500 rpm and the supernatant was applied to a Ni-NTA resin equilibrated with 50 mM $KH_2PO_4$ pH 7.5, 300 mM KCl, 10% glycerol, and 10 mM imidazole. After extensive washing, the protein was eluted with the same buffer containing 300 mM imidazole. The eluate was concentrated in an Amicon centriprep-10 and applied to a Sephacryl-300 column equilibrated with 20 mM Tris-HCl pH 7.5, 200 mM NaCl, 5% glycerol, and 5 mM DTT.

***Curve-fitting of fluorescence binding and competitive-displacement experiments.*** Binding isotherms from fluorescence anisotropy experiments were fit with the following form of the quadratic binding equation, which describes a non-cooperative 1:1 binding equilibrium based on total ligand concentration ($[L_t]$), total nominal protein concentration ($[R_t]$), the dissociation constant ($K_d$), and stoichiometery (s – the ratio of active ligand-binding sites to estimated protein concentration):

$$Y = B + \Delta(s/2[L_t])\left((K_d/s) + ([L_t]/s) + x - \sqrt{\begin{array}{l}(K_d/s)^2 + ([L_t]/s)^2 + x^2 \\ +2(K_d/s)([L_t]/s) + 2(K_d/s)x - 2([L_t]/s)x\end{array}}\right)$$

In this equation, *B* represents the anisotropy of the unbound ligand, Δ its change upon binding to the protein, and *x* the nominal concentration of SecA determined using its extinction coefficient to quantify the concentration of the protein stock solution after dilution into 6 M guandine-HCl, 20 mM sodium phosphate, pH 6.5. The value of $[L_t]$ was fixed to the concentration of MANT-labeled nucleotide used in the experiment, as determined using its extinction coefficient to quantify the concentration of its stock solution. The parameters *B*, Δ, *s*, and ($K_d/s$) were fit using the Marquardt-Levenberg algorithm as implemented in the program PRISM 5.0d (Graphpad Inc., San Diego, CA). The ratio ($K_d/s$) was fit as a single parameter to improve stability, and the uncertainty in this parameter and *s* were propagated into that of their product (*i.e.*, $K_d$). Stability was improved further by sharing the parameter Δ for series of experiments performed at comparable times and the parameter *s* for experiments performed using the same protein stock solution. For some experiments in which the concentration of the MANT-labeled nucleotide was less than the $K_d$ value, fitting of *s* was unstable, in which case it was fixed to 1.0. The optimized value of *s* was always between 0.8 and 1.2 when it could be fit stably. In kinetic displacement experiments, a saturating concentration of 5-25 mM SecA was incubated with 900 nM Mg-MANT-ADP or Mg-MANT-ATP for 4 minutes, and exchange was initiated by adding an excess 10 mM of unlabeled Mg-ADP. At the end of each experiment, excess EDTA was added to trigger release of any MANT-labeled nucleotide that remained bound to the protein. Fluorescence data were monitored continuously during additions, and the data were analyzed in PRISM 5.0d using the following equation:

$$Y = MIN + (MAX - MIN)\exp(-k(t - t0)/60.0)$$

The parameter *MAX* represents the initial signal from the MANT-labeled nucleotide, *MIN* its final value at the end of the displacement process, *k* the kinetic rate constant, and *t0* the time of addition of the competing ligand. All four parameters were fit simultaneously using the Marquardt-Levenberg algorithm, with the optimization of *MAX* explicitly assuming the signal prior to time *t0* to have this value. On-rates were determined by measuring the kinetic rate constant for binding ($k_{on\text{-}obs}$) at different SecA concentrations and 60 nM Mg-MANT-ADP or Mg-MANT-ATP, and the value of $k_{on}$ was inferred from the slope in a linear least-squares regression of $k_{on\text{-}obs}$ *vs.* [SecA]. See Fak *et al.* [2] for further explanation of this procedure.

***Protein crystallization and refinement.*** Crystals were grown in 54.5% $Am_2SO_4$, 31% glycerol, and 20 mM BES pH 7.0 at 26 ºC, and the mother liquor also served as the cryoprotectant. Crystals were harvested in liquid propane and stored in liquid nitrogen. Data were collected at the Advanced Photon Source at Argonne National Laboratory in Argonne, IL and at the National Synchrotron Light Source at Brookhaven National Laboratory in Upton, NY. The structures were solved by molecular replacement using 1M6N as a model to a resolution of 3.4 Å for E208Q-*Bs*SecA (PDB accession number 3IQM) and 3.3 Å for E208Q R489K-*Bs*SecA (3IQY).

***Isothermal titration calorimetry.*** Experiments were performed on a Microcal VP-ITC or $ITC_{200}$ (GE Healthcare, Piscataway, NJ) and analyzed using Origin 7.0 for ITC (OriginLab, Northampton, MA). Proteins were dialyzed into 1 L TKM buffer using 3.5-10K Slide-A-Lyzer dialysis cassettes overnight. Following two subsequent buffer exchanges, the final buffer was used to make Mg-ADP stocks. Mg-ADP was resuspended in the final TKM dialysis buffer, and the pH was adjusted to be within 0.05 pH units of the buffer, typically near pH 8.0. 10-40 μM protein was used with 100-800 μM Mg-ADP at 25 ºC, and 1 μM Mg-ADP was injected in 4 μl volumes that were 4 minutes apart after an initial delay of 5 minutes, with a stirring speed of 290 rpm. Injections were performed until saturation occurred and only the heat of dilution was being measured.

***Differential scanning calorimetry.*** Experiments were performed on 10-20 μM SecA ± 1 mM Mg-ADP in TKM buffer on a Microcal VP-DSC (GE Healthcare, Piscataway, NJ) and analyzed using Origin 7.0 for DSC. Proteins and nucleotide stocks were prepared identically to ITC experiments. Scans were conducted from 20-60 ºC at 1 ºC/min after an initial equilibration step at 20 ºC for 30 min. Equivalent scans conducted on buffer alone (*vs.* buffer in the reference cell) were subtracted to yield background-corrected data for analysis and display.

***Hydrogen-deuterium exchange mass spectrometry.*** Amide $^1H/^2H$ exchange experiments were conducted as described in Sharma *et al.* [3] with slight modifications. A 5 □l aliquot of the SecA variant at ~1 mg/ml in non-deuterated TKM buffer (pH 8.0) was mixed with 15 □l of the same buffer made in deuterated water (*i.e.*, with $^2H_2O$). After being incubated at the indicated temperature for the indicated periods of time (Fig. 9), exchange reactions were quenched by adding 30 □l of a non-deuterated solution containing 1.0 M Gu-HCl and 0.5% formic acid and then snap-freezing on dry ice prior to storage at -80 ºC. For the zero-time-point, the 5 □l of protein was mixed with 15 □l of non-deuterated TKM buffer (pH 8.0). System back-exchange was calibrated via a nominally fully deuterated protein sample incubated in 1M TCEP in deuterated water for 60 hours at 4 ºC. Proteolysis on an immobilized pepsin column followed by reversed-phase chromatography in an aceonitrile gradient on a C18 column and mass spectrometric data acquisition/analysis on an LTQ electrospray linear ion-trap mass spectrometer (ThermoFisher, Waltham, MA) were all performed as described [3].

# Supporting References

(1) Weinkauf, S.; Hunt, J. F.; Scheuring, J.; Henry, L.; Fak, J.; Oliver, D. B.; Deisenhofer, J. Acta Crystallogr D Biol Crystallogr 2001, 57, 559.

(2) Fak, J. J.; Itkin, A.; Ciobanu, D. D.; Lin, E. C.; Song, X. J.; Chou, Y. T.; Gierasch, L. M.; Hunt, J. F. Biochemistry 2004, 43, 7307.

(3) Sharma, S.; Zheng, H.; Huang, Y. J.; Ertekin, A.; Hamuro, Y.; Rossi, P.; Tejero, R.; Acton, T. B.; Xiao, R.; Jiang, M.; Zhao, L.; Ma, L. C.; Swapna, G. V.; Aramini, J. M.; Montelione, G. T. Proteins 2009.

(4) Drenth, A. Principles of Protein X-Ray Crystallography; Springer-Verlag: New York, 1994.

(5) Otwinowski, Z., Minor, W. Methods Enzymol 1997, 279, 307.

(6) Acta Crystallogr D Biol Crystallogr 1994, 50, 760.

(7) Story, R. M.; Li, H.; Abelson, J. N. Proc Natl Acad Sci U S A 2001, 98, 1465.

(8) Kim, D. M., Columbia University, 2009.

(9) Hunt, J. F.; Weinkauf, S.; Henry, L.; Fak, J. J.; McNicholas, P.; Oliver, D. B.; Deisenhofer, J. Science 2002, 297, 2018.

(10) Ulbrandt, N. D.; London, E.; Oliver, D. B. J Biol Chem 1992, 267, 15184.

# Figure S2

## Table S1. Crystallographic data for *Bs*SecA mutants.

| | E208Q-*Bs*SecA [a] | E208Q R489K-*Bs*SecA |
|---|---|---|
| **Space Group** | $P3_112$ | $P3_112$ |
| **Cell parameters (Å)** | 130.1, 130.1, 153.9 | 131.0, 131.0, 152.0 |
| **Resolution (Å)** | 3.4 | 3.3 |
| **Number of reflections** | 16,394 | 19,062 |
| **Mean redundancy** | 3.4 | 7.9 |
| **$\langle I/s_I \rangle$** | 14.9 (2.5) | 22.8 (2.9) |
| **$R_{sym}$ (%)** | 7.4 (43.9) | 9.1 (68.3) |
| **Completeness (%)** | 93.5 (95.7) | 100.0 |
| **X-ray source** | NSLS X25 | NSLS X12B |
| **$R_{work}$ (%)** | 20.9 | 20.7 |
| **$R_{free}$ (%)** | 26.7 | 26.9 |
| **Rmsd in bond lengths (Å)** | 0.011 | 0.011 |
| **Rmsd in bond angles (°)** | 1.3 | 1.3 |
| **Model contents:** | | |
| ***Protein residues*** | 1-802 | 1-802 |
| ***Ligands*** | 11 sulfates | 4 sulfates |
| **Ramachandran distribution:** | | |
| ***Core*** | 79.1 | 84.0 |
| ***Additionally allowed*** | 20.1 | 15.3 |
| ***Generously allowed*** | 0.8 | 0.7 |
| ***Disallowed*** | 0.0 | 0.0 |
| **PDB accession code:** | 3IQM | 3IQY |

**[a] Standard definitions were used for all parameters [4]. Data reduction and refinement statistics come from SCALEPACK [5] and CNS [6], respectively. The numbers in parenthesis are for the highest resolution shell.**

## Figure S1

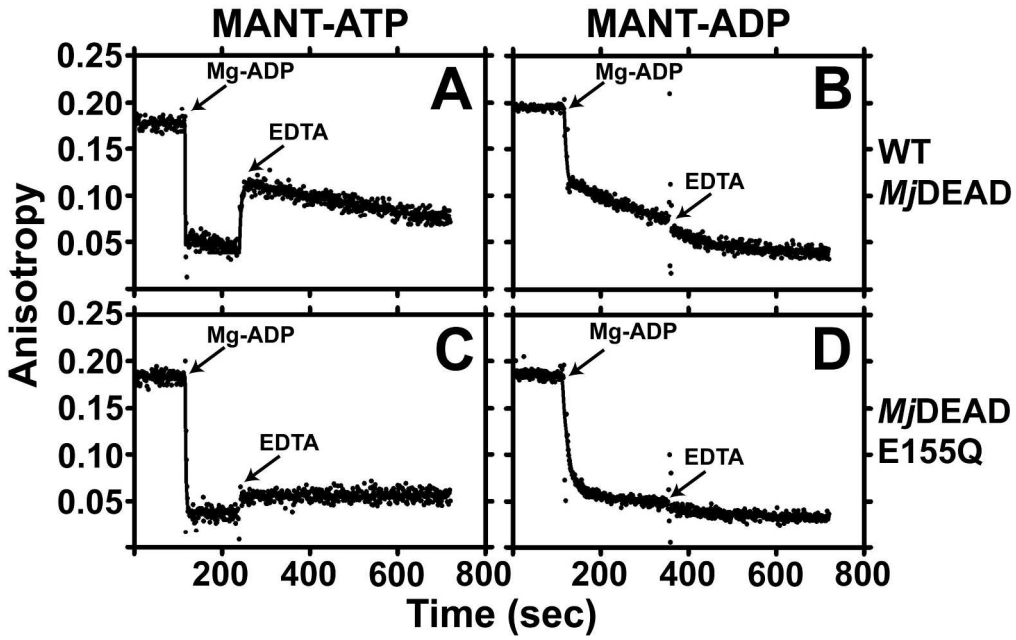


***Figure S1. The E-to-Q mutation in the catalytic base of a model DEAD-box helicase fails to kinetically trap MANT-ATP.*** The MJ0669 protein (*Mj*DEAD), a DEAD-box helicase from the *Methanococcus jannaschii*, previously had its crystal structure determined without bound nucleotide [7]. *Mj*DEAD variants without (top) and with the E155Q mutation in the catalytic glutamate (bottom) were purified using a genetically engineered C-terminal hexahistidine affinity tag, and the rates at which they release MANT-ATP (left) or MANT-ADP (right) were analyzed at 25 ˚C using the fluorescence anisotropy assay shown in Fig. 3 in the main text. Purified enzymes were added at 8 μM concentration to 900 nM MANT-nucleotide and an equal concentration of $MgCl_2$ in a buffer containing 50 mM KCl, 20 μM EDTA, 1.0 mM LiCl, 25 mM Tris-Cl, pH 7.6. Release of the MANT-labeled nucleotide was initiated by addition of 10 mM unlabeled Mg-ADP at the indicated time, followed later by the addition of 10 mM EDTA. LiCl was included in the assay buffer because $Na^+$ or $Li^+$ was observed to be required for high-affinity ATP binding to *Mj*DEAD, and $Li^+$ promoted somewhat tighter binding than $Na^+$ [8]. An extensive set of nucleotide-binding experiments provided some evidence that the protein, which was purified as a monomer in high-salt buffer, forms a dimer with two cooperatively coupled nucleotide-binding sites in low the low-salt buffer used in the assays shown here [8]. **A)** All bound MANT-ATP is released very rapidly from WT *Mj*DEAD, although partial rebinding is promoted by addition of EDTA to chelate $Mg^{2+}$. **(B)** Approximately half of bound MANT-ADP is released very rapidly by WT-*Mj*DEAD, while the other half is released slowly. This behavior indicates different kinetics of nucleotide release from different subunits in the population, possibly from two subunits in a conformationally asymmetrical dimer. Addition of EDTA to chelate $Mg^{2+}$ modestly accelerates MANT-ADP release from the kinetically occluded binding site. **(C)** MANT-ATP is also released very rapidly from E155Q-*Mj*DEAD, demonstrating that this mutation in the catalytic glutamate does not kinetically trap MANT-ATP in the active site. Compared to the WT enzyme, E155Q-*Mj*DEAD rebinds only a small amount of MANT-ATP upon addition of EDTA to chelate $Mg^{2+}$. **(D)** In contrast to the behavior exhibited by the WT enzyme, all bound MANT-ADP is released very rapidly from E155Q-*Mj*DEAD, indicating that the mutation prevents formation of the kinetically occluded MANT-ADP complex formed by the WT enzyme.

# Figure S2

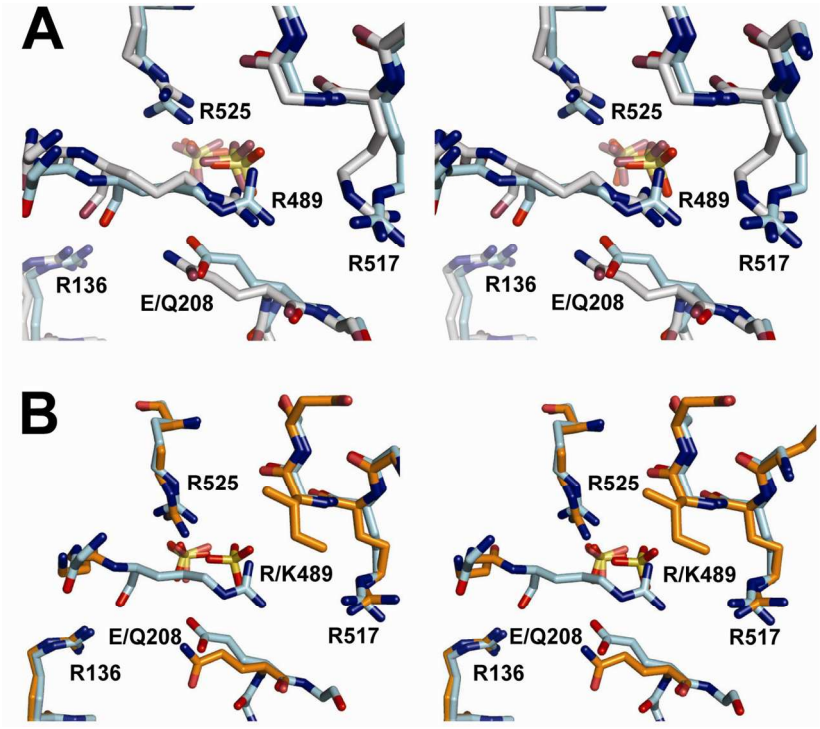


***Figure S2. Crystal structures of E208Q-BsSecA and E208Q-R489K-BsSecA show minor changes in active-site stereochemistry.*** The stereopairs show the active site region after least-squares superposition of *apo* crystal structures (Table S1) of E208Q-*Bs*SecA *vs.* WT-*Bs*SecA (panel A) or E208Q-R489K-*Bs*SecA *vs.* WT-*Bs*SecA (panel B). The WT structure (PDB id 1M6N) is shown in light cyan, while the E208Q structure is shown in gray and the E208Q-R489K structure is shown in orange. Nitrogen and oxygen atoms are colored blue and red, respectively, while bound sulfate molecules are shown in orange and red. Crystals were grown at 26 ˚C in 54.5% ammonium sulfate, 31% glycerol, and 20 mM BES, pH 7.0 [9].

## Figure S3

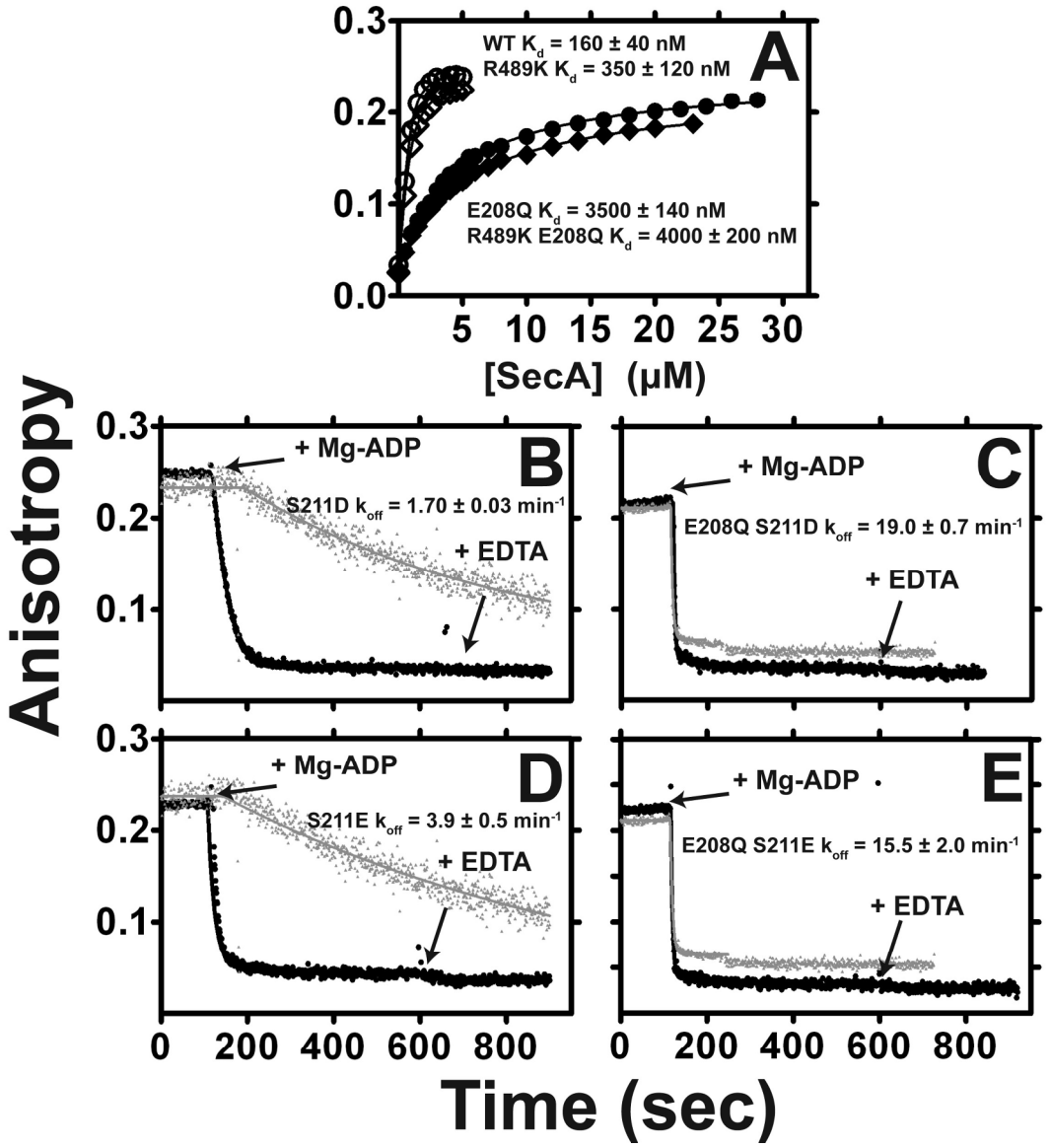


***Figure S3. Restoration of active-site charge balance does not restore nucleotide-binding affinity or decrease the nucleotide-release rate caused by the E-to-Q mutation.*** Fluorescent anisotropy experiments using MANT-labeled nucleotides were used to evaluate the nucleotide binding affinity and release kinetics of R489K mutations in WT and E208Q-*Bs*SecA in KEMT buffer (pH 7.6). Binding experiments (panel **A**) were conducted at 25 ˚C using equivalent methods to Fig. 2, while release experiments (panels **B**-**E**) were conducted at 5 ˚C using equivalent methods to Fig. 3. The table shows thermodynamic and kinetic parameters derived from curve-fitting of the data shown in the display panels. **(A)** *Bs*SecA was titrated onto 900 nM Mg-MANT-ADP; results are shown for WT (○), E208Q (●), R489K (◊), and E208Q-R489K (♦) variants. **(B-E)** The black anisotropy traces show release of MANT-ADP after addition of 10 mM unlabeled Mg-ADP to S211D (panel **B**), E208Q-S211D (panel **C**), S211E (panel **D**), or E208Q-S211E (panel **E**) variants. The equivalent data from the WT (panels **B** and **D**) and E208Q (panels **C** and **E**) enzymes are shown in gray for comparison.

## Figure S4

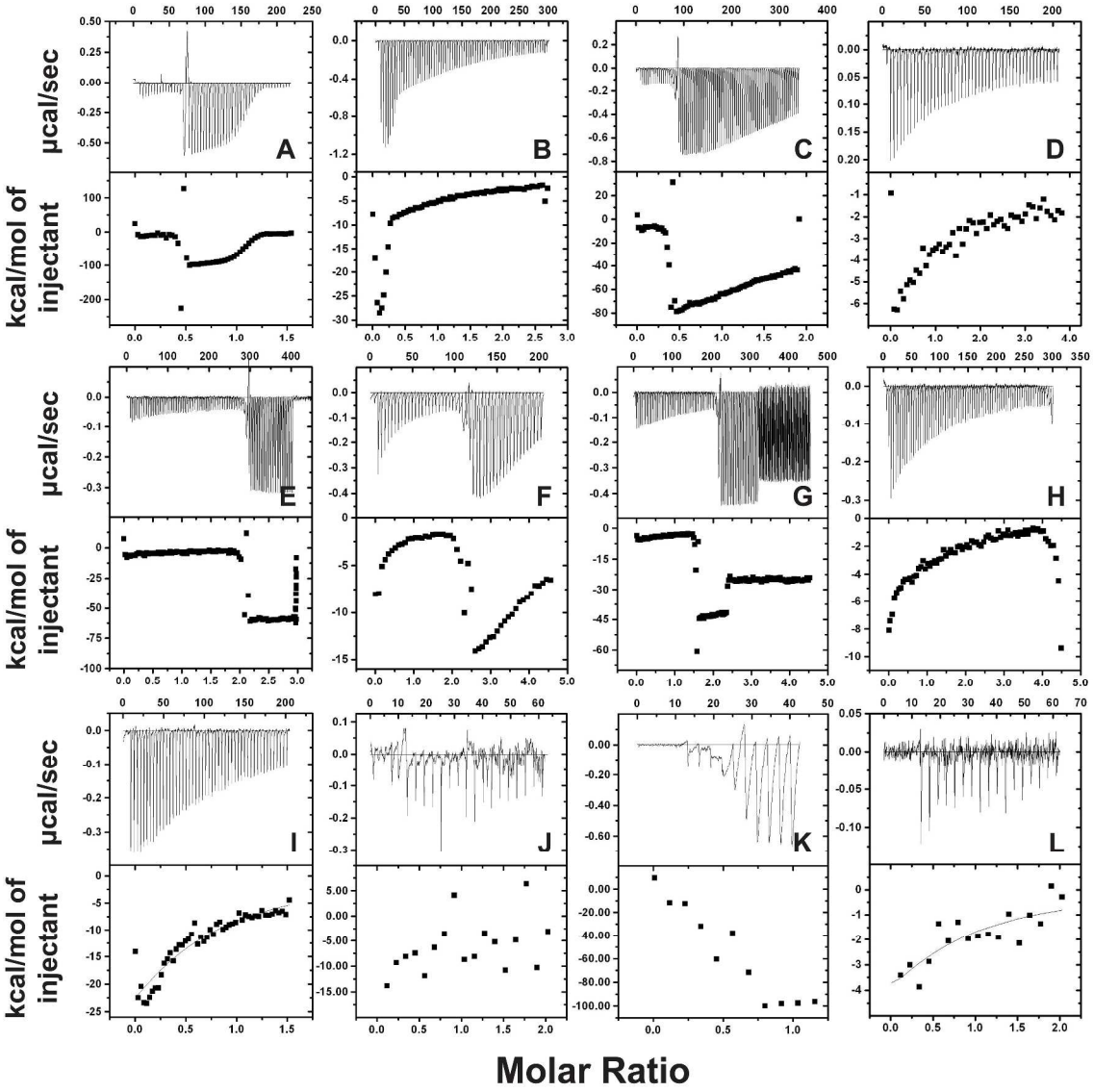


***Figure S4. E210Q-EcSecA behaves erratically in ITC experiments.*** ITC experiments generated readily interpretable data for WT-*Bs*SecA, E208Q-*Bs*SecA, and WT-*Ec*SecA that also correlated with measured fluorescence data (Table 1). However, ITC experiments performed on E210Q-*Ec*SecA were consistently uninterpretable and irreproducible, showing a sudden change in heat release at an arbitrary point in the titration. A representative sampling of experimental data is shown here. Similar pathologies were observed over the course of several years, irrespective of enzyme or ligand preparation, protein or ligand concentration, or the model of the ITC instrument (VP-ITC or $ITC_{200}$). This specific mutant protein seems likely to adhere to the wall of the sample cell, which is coated with an inert metal alloy (Hastelloy®) designed to have a high degree of chemical resistance, and then be released after crossing a critical threshold in Mg-ADP concentration during the titration. **(A-H)** Experiments run on different E210Q-*Ec*SecA samples using a VP-ITC in the Keck Biotechnology Resource Center at Yale University. **(I)** Experiment run on an E210Q-*Ec*SecA sample on a VP-ITC in the Department of Chemistry at Rutgers University. **(J-L)** Experiments run on different E210Q-*Ec*SecA samples using an $ITC_{200}$ in the laboratory of Charalampos Kalodimos at Rutgers University.

# Figure S5

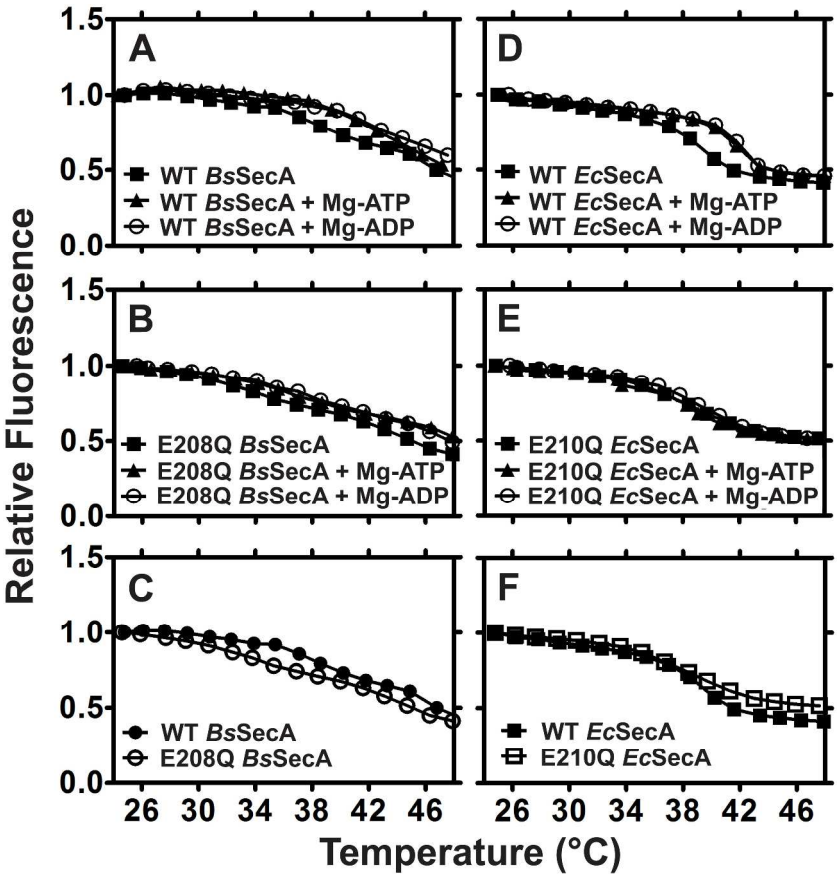


***Figure S5. Thermal titrations monitored using intrinsic tryptophan (trp) fluorescence show that the E208Q mutation lowers the temperature of the ECT in BsSecA.*** The ECT can be monitored in both *Ec*SecA [9,10] and *Bs*SecA [1] based on changes in the fluorescence quantum yield of trp residues buried in the conformational ground state but more solvent-exposed in the high-temperature conformation. The thermal titrations shown here were conducted as previously described [2,9] on 250 nM SecA in the absence or presence of 20 μM Mg-ADP or Mg-ATP in KEMT buffer (pH 7.6). **(A)** WT-*Bs*SecA. Addition of either nucleotide produces a clear increase in the $T_m$ of the ECT as monitored by trp fluorescence. **(B)** E208Q-*Bs*SecA. Nucleotide addition produces at most a modest increase in the apparent $T_m$. **(C)** Comparison of titrations of WT-*Bs*SecA (panel **A**) and E208Q-*Bs*SecA (panel **B**) in the absence of nucleotide; the shift in the fluorescence *vs.* temperature profile suggests that the E208Q mutation facilitates the ECT, as proven by DSC (Figs. 8 & S5). **(D)** WT-*Ec*SecA. Addition of either nucleotide to the wild-type enzyme again produces a clear increase in the $T_m$ of the ECT as monitored by trp fluorescence. **(E)** E210Q-*Ec*SecA. Nucleotide addition fails to produce an increase in the apparent $T_m$, consistent with a substantial reduction in nucleotide binding energy due to the mutation (Table 1). **(F)** Comparison of titrations of WT-*Ec*SecA (panel **D**) and E210Q-*Ec*SecA (panel **E**) in the absence of nucleotide; the similarity in the profiles is consistent with other data (*e.g.*, Figs. 8-9) indicating that the E-to-Q mutation in the catalytic base has a more subtle effect on the conformational properties of *Ec*SecA compared to *Bs*SecA.

# Figure S6

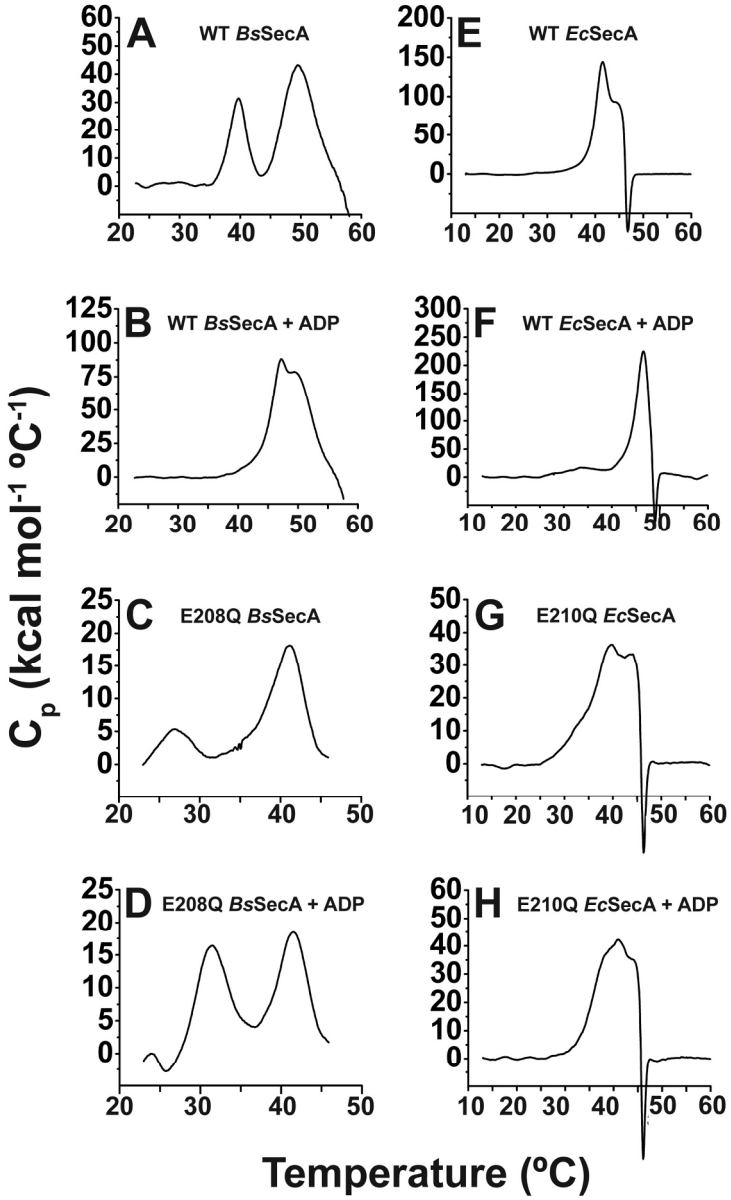


***Figure S6. Differential scanning calorimetry (DSC) of WT and E-to-Q BsSecA and EcSecA.*** The DSC data are shown here again to enable clear visualization of the details in each experiment. With respect to Fig. 7 in the main text, the same data are re-plotted with the enthalpy axis autoscaled for each individual experiment. DSC scans were conducted at 1 ˚C per minute in TKM buffer (pH 8.0). (A,B) 10 μM WT-*Bs*SecA without (panel A) or with (panel B) 1 mM Mg-ADP. (C,D) 20 μM E208Q-*Bs*SecA without (panel C) or with (panel D) 1 mM Mg-ADP. (E,F) 10 μM WT-*Ec*SecA without (panel E) or with (panel F) 1 mM Mg-ADP. (G,H) 20 μM E210Q-*Ec*SecA without (panel G) or with (panel H) 1 mM Mg-ADP. The broad shoulder preceding the main transition in panel G seems likely to represent a series of sequential local conformational changes in E210Q-*Ec*SecA.